

Memory consolidation drives the enhancement of remote cocaine memory via prefrontal circuit

Lin Lu (✉ linlu@bjmu.edu.cn)

Peking University Sixth Hospital <https://orcid.org/0000-0003-0742-9072>

Xiaoxing Liu

Tangsheng Lu

Xuan Chen

Shihao Huang

Wei Zheng

Wen Zhang

Peking University

Shi-Qiu Meng

Wei Yan

Peking University <https://orcid.org/0000-0002-5866-6230>

Le Shi

Institute of Mental Health/National Clinical Research Center for Mental Disorders/Peking University
Sixth Hospital <https://orcid.org/0000-0003-4750-3492>

Yanping Bao

Peking University <https://orcid.org/0000-0002-1881-0939>

Yan-Xue Xue

Jie Shi

Peking University <https://orcid.org/0000-0001-6567-8160>

Kai Yuan

<https://orcid.org/0000-0002-3498-8163>

Ying Han

National Institute on Drug Dependence, Peking University <https://orcid.org/0000-0002-8381-4071>

Article

Keywords:

Posted Date: September 22nd, 2023

DOI: <https://doi.org/10.21203/rs.3.rs-3174594/v1>

License: © ⓘ This work is licensed under a Creative Commons Attribution 4.0 International License.

[Read Full License](#)

Additional Declarations: The authors have declared there is **NO** conflict of interest to disclose

Version of Record: A version of this preprint was published at Molecular Psychiatry on January 15th, 2024. See the published version at <https://doi.org/10.1038/s41380-023-02364-w>.

Abstract

Remote memory usually decreases over time, whereas remote drug-cue associated memory exhibits enhancement, increasing the risk of relapse during abstinence. Memory system consolidation is a prerequisite for remote memory formation, but neurobiological underpinnings of the role of consolidation in the enhancement of remote drug memory are unclear. Here, we found that remote cocaine-cue associated memory was enhanced in rats that underwent self-administration training, together with a progressive increase in the response of prelimbic cortex (PrL) CaMK neurons to cues. System consolidation was required for the enhancement of remote cocaine memory through PrL CaMK neurons during the early period post-training. Furthermore, dendritic spine maturation in the PrL relied on the basolateral amygdala (BLA) input during the early period of consolidation, contributing to remote memory enhancement. These findings indicate that memory consolidation drives the enhancement of remote cocaine memory through a time-dependently increase in activity and maturation of PrL CaMK neurons receiving a sustained BLA input.

INTRODUCTION

Forming memories are essential for survival, guiding our behaviors based on past experience. The expression of most these memories typically gradually weakens over time as an adaptive process of forgetting¹. Whereas, in some types of maladaptive memories, such as the drug-cue associated memories which account for the risk of drug relapse², their expression is progressively enhanced from recent memory to remote one during prolonged time³. The formation of remote memory depends on system-level of memory consolidation, during which specific brain regions undergo reorganization, with subcortical areas responsible for recent memory and the neocortex involved in permanent storage of remote memory⁴. Previous studies have reported that memory enhancement can be modulated through reconsolidation process⁵, but we have a limited understanding of the neural underpinnings about enhancement of remote drug-cue associated memory through system consolidation.

The prelimbic division of the medial prefrontal cortex (PrL) has been increasingly shown to be important for the consolidation of remote memory. Numerous studies have identified that the PrL can function as a storage hub of remote memory, and this role gradually gets matured during the system consolidation process, evidenced by the specific reactivation by remote but not recent memory expression^{6,7}. Furthermore, this functional maturation of PrL required dense upstream inputs, such as from the basolateral amygdala (BLA) and hippocampus⁶⁻⁸. Optogenetically silencing projections from the hippocampus or amygdala effectively dampened synaptic plasticity of the prefrontal cortex, attenuating the expression of remote memory^{6,9}. Although these studies identified the contribution of PrL to consolidation of remote memory, whether the enhancement of remote drug-cue associated memory is established through the PrL during system consolidation has far been unknown. Of these broad upstream inputs, the BLA has shown greater potential in modulating drug-cue associated memory^{10,11}. However, it remains to be determined whether and how the BLA input participates in the enhancement of remote drug

memory via assisting the PrL. In this study, we found that the enhancement of remote cocaine memory resulted from memory system consolidation via a stepwise increase in response to cues and mature dendritic spines in the PrL, which depended on the BLA projection during an early period of system consolidation.

MATERIALS AND METHODS

Animals

Male Sprague-Dawley rats (weighing 280–300 g upon arrival) were purchased from Vital River Laboratories. The rats were housed five per cage for 2 weeks before the experiments and then were individually housed after virus delivery or self-administration surgery. All rats were maintained on a reverse 12 h/12 h light/dark cycle (lights on at 8:00 AM) with free access to food and water. All animal procedures were performed in accordance with the National Institutes of Health Guide for the Care and Use of Laboratory Animals and approved by the Biomedical Ethics Committee for animal use and protection of Peking University.

Surgery

Self-administration surgery was performed as described previously^{12,13}. The rats were anesthetized with isoflurane (4–5% for induction; 1.5–2% for maintenance). Silastic catheters were inserted in the jugular vein, passed to the midscapular region, and attached to a cannula. To sterilize the catheters and keep them clear, we injected penicillin (North China Pharmaceutical Group Corporation, 80 U/mg, dissolved in 0.2% heparin sodium at 0.25 mg/mL) in the cannula daily until the end of self-administration training.

For calcium imaging, AAV-CaMK α -GCaMP6s-WPRE-hGH polyA (AAV2/9, $\geq 2.00 \times 10^{12}$ vector genome/mL) was unilaterally injected in the PrL or BLA (300 nl/side). For the chemogenetic inhibition of PrL and BLA CaMK neurons, AAV-CaMK α -hM4D(Gi)-mCherry-WPRE polyA (AAV2/9, 1.00×10^{13} vector genome/mL) and AAV-CaMK α -mCherry-WPRE polyA (AAV2/9, 1.0×10^{13} vector genome/mL) were diluted with phosphate-buffered saline (PBS) at a ratio of 1:1 and injected in the PrL (500 nl/side) or BLA (300 nl/side). For chemogenetic inhibition of the BLA→PrL or BLA→IL glutamatergic projection, we injected retroAAV-hSyn-GFP-Cre-WPRE polyA (AAV2/R, 1.0×10^{13} vector genome/ml) in the PrL (400 nl/side) or IL (250 nl/side) and AAV-CaMK α -DIO-hM4D(Gi)-mCherry-WPRE-hGH polyA (AAV2/9, 1.00×10^{13} vector genome/mL) in the BLA (300 nl/side). For detecting the dendritic spine in the PrL CaMK neurons receiving BLA input along with the inhibition of BLA CaMK neurons, AAV-CaMK α -DIO-EGFP-WPREs (AAV2/8, 5.81×10^{12} vector genome/mL) was injected into the PrL (300nl/side), and a mixture of AAV-hSyn-Cre-WPRE-hGH polyA (AAV2/1, 1.04×10^{13} vector genome/ml) and AAV-CaMK α -hM4Di-mCherry-WPRE polyA (AAV2/9, 5.81×10^{12} vector genome/mL or 1.04×10^{13} vector genome/ml) was injected in the BLA (1:1 ratio, total of 500 nl/side).

Virus was injected in the PrL (anterior/posterior, + 3.2 mm, medial/lateral, \pm 0.5 mm; dorsal/ventral, -4.0 mm), BLA (anterior/posterior, + 2.3 mm; medial/lateral, \pm 5.2 mm; dorsal/ventral, -8.6 mm), or IL (anterior/posterior, + 3.3 mm; medial/lateral, \pm 0.6 mm; dorsal/ventral, -5.3 mm). All viruses were purchased from BrainVTA (Wuhan, China). We injected the virus (1 nL/s) bilaterally in the BLA, PrL, or IL using 10 μ L microsyringes (Shanghai Gaoge Industrial and Trading Co., Ltd) that were connected to a borosilicate glass capillary. The syringes were connected to a nanoliter microinjection pump (World Precision Instruments) that was controlled by SYS-Micro4 (World Precision Instruments). To prevent virus from diffusing to adjacent brain regions, we maintained the glass capillary for 5 min after insertion and held it for an additional 10 min after the injection.

Retrograde tracing

For retrograde RV tracing of the monosynaptic input to PrL CaMK α neurons, a mixture of AAV-CaMK α -Cre-WPRE-hGH polyA (AAV2/9, 5.22×10^{12} vector genome/ml), AAV-EF1 α -DIO-mCherry-F₂A-TVA-WPRE polyA (AAV2/8, $\geq 2.00 \times 10^{12}$ vector genome/ml), and AAV-EF1 α -DIO- Δ RVG-WPRE-hGH polyA (AAV2/8, $\geq 2.00 \times 10^{12}$ vector genome/ml) was injected in the PrL in wildtype rats (1:1:1 ratio, a total of 600 nL). 3 weeks later, RV-EnvA- Δ G-EGFP (300 nL, $\geq 2.00 \times 10^8$ IFU/ml) was injected at the same coordinates under the same conditions. The injection method was the same as for virus delivery. We used the Zeiss LSM880 with Airyscan with a 40 oil-immersion objective for imaging.

Fiber photometry

During the memory test, we recorded the fluorescence signal of the CaMK α neurons in the PrL or BLA, using a standard 405/470-nm multi-channel fiber photometry device (Inper Technology, Hangzhou, Zhejiang province, China). A 470nm laser was used to excite GCaMP fluorescence signals to measure the Ca²⁺ activity of BLA/PrL neurons, and 405nm laser served as a control for movement artifacts and fluorescence bleaching. As an appropriate acquisition parameter, the intensity of the laser at the tip of fiber was adjusted to 20–40 μ W, and the signal was recorded at 50Hz. All data were analyzed using custom programs written in Python. To process Ca²⁺ signals, baseline correction and motion-correction strategies were employed. The 405nm trace was subtracted from the 470nm trace using a least-squares regression approach. Then we sorted the recorded data by behavioral trials. For each trial, data were collected between the first and last 10 s of the cue onset. For each trial, Delta F/F ratio = (470 signal – 405 signal) / 405 signal¹⁴. Graphs and heatmaps were generated in the jupyter notebook by plotting data 10 s before and after cue onset. The AUC was calculated in the jupyter notebook by sklearn.metrics auc function data 10 s before and after cue onset. The trial data were aligned with the cue exposure and presented as an average trace, with shaded areas indicating standard error mean (SEM) fluctuations.

Cocaine self-administration training

Self-administration chambers were equipped with two transparent organic glass walls, two gray aluminum walls, and a steel grid floor. There was one left nosepoke hole and one right nosepoke hole positioned 5 cm above the grid floor. When the rat put its nose in the left nosepoke hole, it would receive a

cocaine infusion, simultaneously paired with cues (tone and extinguished light) that remained on for 5 s. We recorded this nosepoke as an “active nosepoke.” A nosepoke in the right hole had no drug or cue consequences and was recorded as an “inactive nosepoke.”

Consistent with our previous research¹⁵, we trained rats for 10 days (some poorly conditioned rats were trained for less than 10 days) to self-administer cocaine HCl (Qinghai Pharmaceutical Factory, dissolved in 5% saline; 0.75 mg/kg/infusion) in six 1-h daily sessions (fixed-ratio 1), separated by a 5 min interval. After an active nosepoke, a 40 s timeout period elapsed, during which no drug was available and no cue was presented. The number of cocaine infusions was limited to 20 per session to prevent overdose. Training began at the beginning of the dark cycle with the presentation of a light. After cocaine self-administration training, the rats were housed in their homecage for abstinence and handled 1–2 times per week. Food and water were freely available.

Memory test

The memory test consisted of a 1 h session. The test conditions were the same as training, including the tone and light, with the exception that an active nosepoke did not trigger cocaine delivery. The test began at the beginning of the dark cycle with the presentation of a light.

Locomotor test

We equipped locomotor chambers (40 cm × 40 cm × 60 cm, JL Behv-LAG-8) with dark walls and a grid floor. A camera was mounted on top of each chamber. An activity monitoring system recorded the distance travelled, time spent in the center area, and velocity. The test lasted 10 min¹⁶.

Chemogenetic manipulation

Clozapine-*N*-oxide (catalog no. HY-17366) was purchased from MedChem Express. Before the intraperitoneal injection, CNO was prepared in 10 mg/mL with dimethylsulfoxide (DMSO) and diluted to 1 mg/mL with saline. For acute chemogenetic intervention, CNO or vehicle (1 mg/kg) was injected intraperitoneally 30 min before the retrieval test. For chronic inhibition, we injected CNO or vehicle (1 mg/kg, i.p.) twice daily (8:00–9:00 AM, 8:00–9:00 PM) because the effect duration of CNO is only 10–11 h¹⁷.

Immunofluorescence

We chose 60 min after the relapse test to measure Fos levels in the brain. After the rats were anesthetized with 20% chloral hydrate, they were perfused with 1× PBS and 4% paraformaldehyde (PFA). Brains were postfixed in 4% PFA for 48 h, followed by dewatering three times with 30% sucrose solution. Brains were then frozen in dry ice and stored at -80°C. Brains were sectioned coronally at 20 μm for immunofluorescence or 30 μm for Nissl staining.

Brain sections were blocked in 5% bovine serum albumin (BSA) in 1× PBS for 1 h at 37°C and incubated overnight at 4°C with rabbit anti-*c-fos* (1:500, Cell Signaling Technology, catalog no. 2250s), mouse anti-

NeuN (1:500, Millipore, catalog no. MAB377B), mouse anti-CaMK (1:500, Abcam, catalog no. ab52476), or mouse anti-GAD67 (1:500, Abcam, catalog no. ab26116) in 5% BSA in 1× PBS. Sections were rinsed in 1× PBS (4 × 5 min) and incubated for 2 h in the dark at room temperature with donkey anti-rabbit Alexa Fluor 488 (1:500, Invitrogen, catalog no. A-21206) and donkey anti-mouse Alexa Fluor 594 (1:500, Invitrogen, catalog no. A-21203). Sections were rinsed in 1× PBS (4 × 5 min) and mounted on glass slides. We used a fluorescence microscope (Olympus, Tokyo, Japan) with a 20× objective lens.

For detecting the c-Fos positive cells, all cell counting was conducted by a researcher who was blind to experimental groups and analyzed using ImageJ software. At least three sections were selected from each brain region for every rat. Cell numbers from the left and right sides of every section were averaged to represent the positive cell numbers for each brain region. The boundaries of each brain region (including the PrL, NAcc, NAcsh, BLA, and dorsal CA1) were outlined as regions of interest according to a rat brain atlas¹⁸. The area was quantified by applying scale calibration. The number of Fos-positive cells was automatically counted by applying a uniform threshold for each section from each brain region. The number of dual Fos-positive/CaMK -positive cells was manually calculated from cells that were selected by ImageJ.

Spine morphometry analysis

The brains were extracted, cut into 50 µm sections, and prepared for confocal microscopy. We used the TCS-SP8 DIVE with a 63 oil-immersion objective (APO CS2 63×, NA = 1.4), a zoom factor of 4, image size (1024 × 1024 pixels, 43.93 × 43.93 µm), with a pinhole set at 1 AU, and a 0.1-µm step size for z-stack image acquisition. Dendritic segments were collected from the secondary or tertiary branches of neurons. We utilized the FilamentTracer module within the Imaris 8 software (Oxford Instruments) to perform three-dimensional reconstructions of dendritic spine morphologies. By utilizing a semi-automated auto-depth function, we analyzed reconstructed dendritic segments with an average length of 20 µm and identified spines. After completing the FilamentTracer creation wizard and generating dendrites and spine objects, all available XTensions are listed under the Tool tab. We used the Imaris Spines Classifier XTension, displaying a list of four default classes: stubby, mushroom, long thin, and filopodial. According to the first rule, all spines with a total length of less than 1 µm are classified as stubby. The second rule states that spines with a mean width of the head greater than the mean width of the neck are classified as mushroom. Long/thin satisfy the third rule, in which the mean width of the neck multiplied by 2 is less than the length of the spine, and the mean width of the neck is less than or equal to the maximum width of the head. All other spines are classified as filopodia¹⁹. One dendrite was analyzed per neuron, and an average of 25 dendrites were analyzed per animal by a blinded rater. The calculation method for delta density was to first calculate the density of dendritic spines (the number of dendritic spines per unit length of dendrite). This value was then divided by the average spine density. The calculation method for delta nosepoke was the number of nosepokes per rat divided by average nosepoke.

Statistical analysis

We used two-sample *t*-tests, Welch's *t*-test, one-way repeated measures analysis of variance (ANOVA) followed by Tukey's multiple-comparison *post hoc* test, Brown-Forsythe and Welch's ANOVAs followed by Dunnett's T3 multiple-comparison *post hoc* test, two-way repeated measures ANOVA followed by the Šídák multiple-comparison *post hoc* test, and two-way ANOVA followed by Tukey's multiple-comparison *post hoc* test for the statistical analyses using GraphPad Prism 9.2 software. We used simple linear regression to analyze the correlation between delta spine density and delta nosepekes. The data are expressed as the mean \pm SEM for continuous variables with a normal distribution. Values of $P < 0.05$ were considered statistically significant.

RESULTS

Enhancement of remote cocaine memory aligns with enhancement of PrL activity to cues

To investigate the dynamics of PrL activity during cocaine memory expression, we employed an extended-access cocaine self-administration model in rats whereby intravenous cocaine was injected and paired with a tone after rats nosepeked in the active hole (Fig. 1a). Similar with previous research³, rats acquired cocaine-cue associated memory following 10 days of self-administration training (Fig. 1b). The expression of cocaine memory was manifested by cue-induced active nosepekes, and this memory test was performed 1, 15, or 30 days after training. The results showed that cue-induced nosepoke behavior increased on day 30 compared with day 1, suggesting the enhancement of remote cocaine memory (Fig. 1c). Next, we assessed whether PrL neurons were activated during recent and remote memory expression. We analyzed the c-Fos levels, a marker of neuronal activation, after the behavioral test. Rats that remained in their homecage and did not undergo the memory test were used as controls (no test group). We found a parallel change in the density of PrL activated cells with cocaine memory expression. After the memory test on day 1 or 15, the number of c-Fos positive cells per mm² did not differ in the test and no test groups. In contrast, the enhancement of remote memory on day 30 markedly increased the density of c-Fos positive cells in the PrL. Additionally, the number of PrL activated cells on day 30 was significantly higher than on days 1 and 15 (Fig. 1d, e). Collectively, these findings indicate that the enhancement of remote cocaine memory can activate the PrL to a greater extent.

We next determined the specific subtype of these PrL activated cells, and detected over an 80% proportion of Ca²⁺ /calmodulin-dependent protein kinase II (CaMK ; a marker of glutamatergic neurons²⁰) in PrL c-Fos positive cells (Fig. S1a, b). Therefore, we assessed the activity of PrL CaMK neurons in recent and remote memory, showing that the density of activated CaMK neurons also showed a time-dependent increase over time (Fig. 1f). Then, to examine the real-time activity of PrL CaMK neurons during memory expression, we performed *in vivo* fiber photometry in rats expressing the adeno-associated virus (AAV)-CaMK -GCaMP6s (Fig. 1g, h). After self-administration training, the Ca²⁺ signal of PrL CaMK neurons was monitored during the test, in which a nosepoke was paired with a 5-s tone (Fig. 1i). The results showed that cue exposure elicited robust increases in Ca²⁺ signals in PrL CaMK neurons during the day

1, 15 and 30 tests (Fig. 1j-p). Additionally, Ca^{2+} signals on days 15 and 30 were both significantly stronger than day 1, whereas Ca^{2+} signals did not differ between days 15 and 30 (Fig. 1q). These results suggest that the activity of PrL CaMK neurons in response to cues time-dependently increases, accompanied by an enhancement of remote cocaine memory.

PrL activity during the early period of consolidation facilitates the enhancement of remote memory

To functionally determine whether PrL CaMK neurons modulate cocaine memory expression, we employed a chemogenetic method to acutely inhibit their activity 1 day (recent memory) and 30 days (remote memory) post-training. AAV-CaMK⁻hM4Di-mCherry was injected in the PrL, thereby causing inhibitory hM4Di designer receptors exclusively activated by designer drugs (DREADD) expression specifically in PrL CaMK neurons (Fig. 2a, b). After self-administration training, clozapine-*N*-oxide (CNO; 1 mg/kg of body weight) or vehicle was administered intraperitoneally 30 min before the test (Fig. 2c-e). We found that the acute inhibition of PrL CaMK neurons did not alter recent memory expression, but it effectively suppressed the expression of remote memory, consistent with previous findings (Fig. 2f)²¹. Notably, the enhancement of remote cocaine memory was markedly attenuated compared with recent one (Fig. 2g). These findings suggest that remote but not recent memory expression relies on PrL CaMK neurons.

Numerous studies reported that the functional contribution of the PrL to remote memory emerged during memory system consolidation^{6,8,22}. Therefore, we hypothesized that the enhancement of remote cocaine memory stems from memory consolidation through strengthening of PrL CaMK neurons activity. To test this hypothesis, we utilized chemogenetic inhibition by injecting CNO (1 mg/kg, i.p.) twice daily to repeatedly suppress the activity of PrL CaMK neurons during system consolidation without affecting the memory expression process (Fig. 2h)^{17,23}. Based on our finding that the pattern of the PrL response to cocaine-related cues was shifted from day 15 (Fig. 1q) and based on previous research^{22,24}, we distinguished an early period (day 1–14 post-training) and late period (day 15–28 post-training) to investigate the influence of PrL CaMK neurons in different consolidation processes on remote memory (Fig. 2i, j). After chronically silencing PrL CaMK neurons during the early period, we found a pronounced decrease in the number of active nosepekes in the CNO group and no change in the number of inactive nosepekes (Fig. 2k-m). An identical manipulation was performed during the late period, whereas the expression of remote cocaine memory on day 30 was not different between the CNO and vehicle groups (Fig. 2n-p). These results indicate that the activity of PrL CaMK neurons during the early, but not late, period of consolidation is necessary for remote cocaine memory enhancement. To exclude the possible confounding effect of the CNO injection itself²⁵, control rats received injections of AAV-CaMK⁻mCherry in the PrL and were trained in the same paradigms, accompanied by administering CNO or vehicle (1 mg/kg, i.p.) during the early period (Fig. S2a-c). The result showed that injections of CNO alone during the early period did not affect active nosepekes on day 30 (Fig. S2d-f). Thus, these collective findings

suggest that memory consolidation contributes to this PrL-involved remote memory enhancement, which is established during the first 2 weeks after training.

The BLA serves as a monosynaptic input to PrL but does not exert a function in memory expression

Our above results demonstrate that memory consolidation promotes the enhancement of remote cocaine memory through a time-dependent increase in the activity of PrL CaMK neurons to cues. Strong evidence indicates that during system consolidation, the PrL requires upstream inputs to drive its function in remote memory^{6, 8}. Therefore, to identify PrL inputs that may contribute to its progressive activity during consolidation, we applied retrograde trans-synaptic labeling to specifically assess the presynaptic targets of PrL CaMK neurons (**Fig. S3a, b**). A mixture of AAV-CaMK α -Cre, AAV-EF1 α -double floxed inverted open reading frame (DIO)-mCherry-TVA, and AAV-EF1 α -DIO- Δ RG was injected into the PrL in wild-type rats. 21 days later, rabies virus (RV)-EnvA- Δ G-enhanced green fluorescent protein (EGFP) was administered in the same location in all animals (Fig. 3a). We detected the co-expression of RV-EGFP and mCherry neurons in the PrL, indicating starter CaMK neurons in the PrL (Fig. 3b, c). Robust EGFP labeling was detected in brain regions with known inputs to PrL CaMK neurons, including the BLA (Fig. 3d), nucleus accumbens core (NAcc; **Fig. S3c**) and shell (NAcsh; **Fig. S3d**), and hippocampus (**Fig. S3e**), demonstrating direct monosynaptic connections to the PrL CaMK neurons.

Among these inputs, we selected the BLA for further investigation because it has been shown to be a hub of processing stimulus-cue associations, and its projection is necessary for the PrL to maintain this association information^{26, 27}. Hence, we first investigated whether the BLA is activated after cocaine memory expression, finding that the density of BLA c-Fos positive cells was increased across every test (**Fig. S4, Fig. S5a, b**). Unexpectedly, although most activated cells in the BLA were CaMK type, no difference in the density of BLA activated CaMK neurons was found over time (**Fig. S5c, d**). Next, to investigate the real-time activity of BLA CaMK neurons during cocaine memory expression, we applied fiber photometry. Our results showed that the Ca²⁺ signals of BLA CaMK neurons were elevated after cue exposure compared with before cue onset (Fig. 3e-j), suggesting that BLA CaMK neurons respond to cocaine-related cues during memory expression²⁸. However, in contrast to observations of PrL CaMK neurons (Fig. 1p, q), we did not find time-dependent changes in Ca²⁺ signals of BLA CaMK neurons to cue from day 1, 15, to 30 (Fig. 3l). Thus, BLA CaMK neurons may stably store information about cocaine-cue associations.

To further elucidate the behavioral function of BLA CaMK neurons in cocaine memory expression, we acutely inhibited BLA CaMK neurons by injecting AAV-CaMK -hM4Di-mCherry in the BLA (Fig. 3m-o). After self-administration training, we found that neither recent nor remote memory expression changed after inhibiting BLA CaMK neurons (Fig. 3p-r). Rats in both the CNO and vehicle group presented enhanced nosepekes in the 30-day test compared with day 1 (Fig. 3s). Altogether, our results indicate that despite the stable response of BLA CaMK neurons to cues is not required for remote cocaine memory enhancement, the BLA may serve as a continual input to the PrL during the consolidation process.

BLA input supports the enhancement of remote memory and PrL spine plasticity during consolidation

Previous evidence suggests that the BLA input during consolidation is critical for supporting PrL function in remote memory⁶. Thus, we hypothesized that the PrL required the BLA projection across system consolidation to facilitate the enhancement of remote cocaine memory. To examine this hypothesis, we injected the retroAAV-hSyn-EGFP-Cre into the PrL and simultaneously injecting the AAV-CaMK α -DIO-hM4Di-mCherry into the BLA, to specifically inhibit BLA CaMK α neurons projecting to the PrL (Fig. 4a-c). After cocaine self-administration training, CNO or vehicle (1 mg/kg, i.p.) was administered twice daily during the early period (Fig. 4d-f). The results showed that the chronic silencing of PrL-projecting BLA CaMK α neurons significantly prevented active nose pokes on day 30 (Fig. 4g). To identify the behavioral specificity of this effect, we assessed the influence of chronically inhibiting the BLA-PrL circuit on exploratory behavior in an open field (Fig. 4h). We found no change in the total distance traveled (Fig. 4i), average velocity (Fig. 4j), or time spent in the center zone (Fig. 4k) between rats received CNO or vehicle during the early period post-training. These findings demonstrate that nonspecific effects on locomotor activity did not account for the attenuation of remote memory when the BLA-PrL circuit was blocked. When CNO or vehicle (1 mg/kg, i.p.) was administered during the late period (Fig. 4l), we observed no change in cocaine memory expression on day 30 (Fig. 4m-o), and no change in any behaviors in the open field apparatus in these rats (Fig. 4p-s).

To further investigate the specific role of the BLA-PrL circuit, we studied the effect of chronically inhibiting the BLA-infralimbic cortex (IL; a region adjacent to the PrL) circuit. RetroAAV-hSyn-EGFP-Cre was bilaterally injected into the IL, and AAV-CaMK α -DIO-hM4Di-mCherry was simultaneously injected in the BLA (Fig. S6a-d). After cocaine self-administration training, the rats received an injection of CNO or vehicle (1 mg/kg, i.p.) during the early period (Fig. S6e, f). The results showed that chronically silencing the BLA-IL circuit had no significant influence on the enhanced remote cocaine memory on day 30 (Fig. S6g). Collectively, these results suggest that the contribution of system consolidation to the enhancement of remote cocaine memory specifically depends on activity of BLA-PrL projection during the early period post-training.

Numerous studies have revealed that PrL function on remote memory results from gradually mature spine plasticity during consolidation, which relies on upstream inputs²⁹. Therefore, we hypothesized that the BLA input may drive PrL function on remote cocaine memory through modulating dendritic spines in the PrL. To visualize the structure of dendritic spines in PrL CaMK α neurons receiving BLA projection, we applied a trans-synaptic anterograde method (Fig. 5a). An anterograde trans-synaptic virus AAV1 was infused with Cre-recombinase, and AAV1-hSyn-Cre was injected in the BLA. Simultaneously, AAV-CaMK α -DIO-EGFP was administered in the PrL, leading to the expression of green fluorescence in PrL CaMK α neurons which received BLA inputs (Fig. S7b). Furthermore, to simultaneously investigate the effect of the BLA projection on PrL spine plasticity during memory consolidation, AAV-CaMK α -hM4Di-mCherry was injected into the BLA in these rats (Fig. S7c). After chronically silencing the BLA CaMK α neurons through

administering CNO or vehicle (1 mg/kg, i.p.) during the early period post-training, rats were sacrificed to detect spines of PrL neurons receiving BLA projection (Fig. 5b-d). We performed high-fidelity three-dimensional reconstruction of dendritic spine morphologies and differentiated various types of spines, including nonmature spines (e.g., filopodia and long thin type) and mature spines (e.g., mushroom type and stubby type; Fig. 5e-g)³⁰. We found that the spine density of PrL neurons receiving BLA input significantly decreased after chronically silencing BLA glutamatergic neurons (Fig. 5h). The stratification of spines by morphological subtype showed that this effect was driven by a selective decrease in filopodia-shaped spines and mushroom-shaped spines (Fig. 5i-l). Next, we examined whether there was a relationship between mushroom-type spines and cocaine memory expression. Through analyzing the correlation between delta spine density and delta nose pokes (calculation see “Materials and methods”), we found a significant positive correlation between mushroom-shaped spines and cocaine memory (Fig. 5m). Altogether, these findings suggest that the maturation of PrL dendritic spines during the early period of consolidation requires the BLA input, thereby facilitating the enhancement of remote cocaine memory.

DISCUSSION

The present study provides compelling evidence that the enhancement of remote cocaine memory is driven by memory system consolidation. Using an extended cocaine self-administration model in rats, we found that remote cocaine-cue associated memory expression exhibited an enhancement. During this process, we observed a time-dependent strengthening of the response of PrL CaMK neurons to cocaine-related cues. Chemogenetic suppression also revealed that memory consolidation drove the enhancement of remote cocaine memory through PrL CaMK neurons, and the early period after training was the major stage for effective intervention. Furthermore, the function of PrL CaMK neurons in remote memory required the BLA input during the early period of consolidation, which can promote the maturation of PrL dendritic spines, mainly mushroom-shaped spines. These data extend previous findings and showed the contribution of system consolidation to the enhancement of remote cocaine memory through PrL CaMK neurons receiving the BLA input (Fig. 5n).

Our results indicate that cocaine-cue associated memory was time-dependently enhanced, but not attenuated, over time, which was different from typical remote memory expression. Notably, a similar phenomenon has been reported in previous findings that cue-induced drug craving (i.e., an intense desire for the effects of a drug) progressively increased during long-term abstinence, which was termed as the incubation of cue-induced drug craving^{31,32}. The incubated drug craving is a critical contributor to drug relapse and generalizes across various drugs³³. Many human studies have identified this phenomenon in individuals with a history of taking nicotine³⁴, methamphetamine³⁵, alcohol³⁶, or cocaine³⁷. Emerging evidence support that drug craving stemmed from past experiences about drug use which can be encoded and stored in memory, suggesting that memory serves as the foundation of drug craving^{2,10,38,39}. Here, our results further demonstrate homogeneity between the enhancement of remote drug-cue associated memory and the incubation of drug craving. Thus, we speculate that the stable memory is a

prerequisite for persistent drug craving during abstinence, and the enhancement of remote drug-cue memory driven by memory consolidation leads to the increased cue-induced drug craving⁴⁰. Although direct evidence is still scarce, many indirect studies have shown that disrupting the memory reconsolidation process can attenuate cue-induced drug craving^{12,39}. Therefore, it is worthy to explore the ways in which the enhancement of drug memories causes an abnormal intensification of drug craving.

Memory system consolidation typically facilitates recent memory to maintain and to turn into stable over time, whereas remote memory tends to become weaker through a process of forgetting¹. In contrast, our data reveal that memory consolidation can drive remote cocaine memory to an abnormal state, that is expression enhancement, similar to previous finding⁵. This kind of remote memory enhancement generalizes to other types of memory, such as the natural reward-cue associated memory⁴¹ and fear memory⁴². Therefore, it is reasonable to suspect that the role of system consolidation in remote memory enhancement is neither attributable to the effect of the additive drug per se, nor correlated with stimulus valence (i.e., appetitive or aversive). One possible factor affecting the function of consolidation is memory strength, in which high-intensity learning would induce stronger expression of remote memory than low-intensity learning⁴³. Here, we applied an extended self-administration training paradigm whereby rats underwent 6-h sessions per day, and every nosepoke can trigger a simultaneous cocaine injection until the maximum number of nosepokes was reached. The strength of association between cocaine and the cue may be a contributor to the increased remote memory expression, due to that the rats which were trained with a rapid infusion rate (5 s), but not a slow (90 s), showed a more pronounced enhancement of remote cocaine memory⁴⁴. Additional findings showed that in rats cue extinction session (repetitive exposure to drug-related cues without injecting the drug) during abstinence reduced the remote drug memory enhancement⁴⁵, possibly due to that extinction session weakened the association between the drug and related cues and blocked the consolidation of drug-cue associated memory. Hence, we hypothesize that the over-strengthened cocaine-cue association during learning would be abnormally consolidated over long periods of time, making behavioral responses to related cues gradually increase. This may explain why individuals with substance use disorders or those who have experienced traumatic events have a higher risk of relapse or suffer from post-traumatic stress disorder^{46,47}. In turn, the early period of consolidation represents a potential time window for blunting remote memory enhancement. Our results showed that chronic inhibition during the early period reduced the cue-induced behavioral response on day 30 post-training. This finding aligns with previous research that the initial 2 weeks post-learning is critical for remote memory²⁴, suggesting the therapeutic value of preventing system consolidation to reduce the drug relapse.

The role of neocortex in remote memory is not fixed but rather undergoes an evolving process during memory system consolidation⁴⁸. Recent investigations have further revealed a time-dependent maturation process of PrL function in memory which required inputs from kinds of brain regions⁶, showing a greater influence on remote memory²². In the present study, we found that the function of PrL glutamatergic neurons on remote cocaine memory enhancement was established during the

consolidation process. This was supported by two key findings. First, we observed an increase in Ca^{2+} signals after cue onset from day 1 to day 30 post-training, indicating a gradually greater ability of the PrL to process the information about cocaine related cues. Consistently, previous findings also showed a pronounced increase in the encoding of related cues information after prolonged abstinence from cocaine⁴⁹. Second, our results revealed that the chronic chemogenetic inhibition of PrL CaMK neurons during the early period significantly reduced the enhancement of remote cocaine memory, in line with previous research that pharmacological inhibition of the PrL decreased the cue-induced behavioral response to cocaine at remote time point²¹.

The BLA serves as a focal point for drug memory⁵⁰, where sensory and emotional signals are processed and integrated⁵¹. Our study found an increase in Ca^{2+} signals in BLA CaMK neurons following exposure to cocaine-related cues. However, unlike the PrL, BLA activity did not show temporal changes during system consolidation, and the acute inhibition of BLA CaMK neurons did not affect the expression of cocaine memory. These results imply that although the BLA may mediate the integration of cocaine and related cues, it is not necessary for the behavioral response to cocaine-related cues. Consistent results were also reported, in which pharmacological inhibition of the BLA had no influence on cue-induced cocaine seeking behaviors at remote time⁵².

Our findings highlight that the sustained input from the BLA to PrL during the early period of consolidation contributes to enhancement of remote cocaine memory, which is consistent with a previous finding that optogenetic inhibition of the BLA-PrL circuit reduced remote fear memory⁶. These processes are accompanied by dynamic dendritic spine plasticity on PrL neurons defined by afferent connections^{29, 53}. Here, we found that blocking the BLA glutamatergic projection during the early period of consolidation decreased dendrite spine density in PrL CaMK neurons receiving BLA input. Among these, the mushroom-shaped spines possibly served as the primary substrate for the elevation of activity of PrL during system consolidation, and appeared to be necessary for the enhancement of remote cocaine memory. This is similar to previous research that PrL neurons displayed more mature and stable synaptic connections during abstinence⁵⁴. Furthermore, the BLA input to PrL also resulted in the transmission of cocaine-cue association information⁵⁵. And this transmission possibly has its behavioral significance that the learned object values encoded by the prefrontal cortex can be retained for at least several months and resistant to interference⁵⁶. Accordingly, we propose that the BLA may function as a cache that integrates the strong association between cocaine and related cues, and during system consolidation BLA can convey this information to PrL for long-term storage. Remarkably, during the early period post-training, more mature and stable dendritic spine plasticity which occurred in PrL neurons receiving BLA input possibly makes the association information abnormally consolidated, inducing stronger response when cue exposure at remote time and leading to enhancement of remote cocaine memory. Following that, the NAcc may be a promising output for investigating the ways in which consolidated cocaine-cue association information flows from the BLA to PrL for persistent storage, and then to downstream regions for directing higher behavioral responses to cues. This is supported by extensive findings that the

optogenetic inhibition of NAcc neurons receiving PrL input can attenuate cue-induced drug seeking at remote⁵⁷.

In summary, we delineated that memory system consolidation drives the enhancement of remote cocaine memory through stepwise mature dendritic spines plasticity and elevated response to cue in PrL neurons receiving BLA input. Importantly, we identified the early period of consolidation as an essential time window for intervention, providing valuable insights into the treatment of drug relapse after prolonged abstinence.

Declarations

ACKNOWLEDGEMENTS

This work was supported by the Chinese National Programs for Brain Science and Brain-like Intelligence Technology (no. 2021ZD0200800), PKU-Baidu Fund (no. 2020BD011), and National Natural Science Foundation of China (no. 81901352). All schematic images were created with BioRender.com.

AUTHOR CONTRIBUTION

L.L., Y.H., X.L., and T.L. designed the study. X.L., T.L., K.Y., X.C., S.H., and W.Zheng performed the experiments. X.L., T.L., Y.H., and Y.B. analyzed the data. X.L. and T.L. prepared the first draft of the manuscript. W.Zhang, S.M., W.Y., L.S., Y.X., J.S., K.Y., Y.H., and L.L. revised the manuscript. All authors read and approved the final version of the manuscript.

COMPETING INTEREST

The authors declare no competing interests.

References

1. Ryan TJ, Frankland PW. Forgetting as a form of adaptive engram cell plasticity. *Nat Rev Neurosci* 2022; 23(3): 173–186.
2. Xue YX, Deng JH, Chen YY, Zhang LB, Wu P, Huang GD *et al*. Effect of selective inhibition of reactivated nicotine-associated memories with propranolol on nicotine craving. *JAMA Psychiatry* 2017; 74(3): 224–232.
3. Wright WJ, Graziane NM, Neumann PA, Hamilton PJ, Cates HM, Fuerst L *et al*. Silent synapses dictate cocaine memory destabilization and reconsolidation. *Nat Neurosci* 2020; 23(1): 32–46.
4. Frankland PW, Bontempi B. The organization of recent and remote memories. *Nat Rev Neurosci* 2005; 6(2): 119–130.
5. Fukushima H, Zhang Y, Archbold G, Ishikawa R, Nader K, Kida S. Enhancement of fear memory by retrieval through reconsolidation. *Elife* 2014; 3: e02736.

6. Kitamura T, Ogawa SK, Roy DS, Okuyama T, Morrissey MD, Smith LM *et al.* Engrams and circuits crucial for systems consolidation of a memory. *Science* 2017; 356(6333): 73–78.
7. Lee JH, Kim WB, Park EH, Cho JH. Neocortical synaptic engrams for remote contextual memories. *Nat Neurosci* 2023; 26(2): 259–273.
8. Dixsaut L, Graff J. Brain-wide screen of prelimbic cortex inputs reveals a functional shift during early fear memory consolidation. *Elife* 2022; 11.
9. Kol A, Adamsky A, Groyzman M, Kreisel T, London M, Goshen I. Astrocytes contribute to remote memory formation by modulating hippocampal-cortical communication during learning. *Nat Neurosci* 2020; 23(10): 1229–1239.
10. Rich MT, Huang YH, Torregrossa MM. Plasticity at thalamo-amygdala synapses regulates cocaine-cue memory formation and extinction. *Cell Rep* 2019; 26(4): 1010–1020.
11. Hsiang HL, Epp JR, van den Oever MC, Yan C, Rashid AJ, Insel N *et al.* Manipulating a "cocaine engram" in mice. *J Neurosci* 2014; 34(42): 14115–14127.
12. Xue YX, Luo YX, Wu P, Shi HS, Xue LF, Chen C *et al.* A memory retrieval-extinction procedure to prevent drug craving and relapse. *Science* 2012; 336(6078): 241–245.
13. Luo YX, Xue YX, Liu JF, Shi HS, Jian M, Han Y *et al.* A novel UCS memory retrieval-extinction procedure to inhibit relapse to drug seeking. *Nat Commun* 2015; 6: 7675–7689.
14. Bruno CA, O'Brien C, Bryant S, Mejaes JI, Estrin DJ, Pizzano C *et al.* pMAT: An open-source software suite for the analysis of fiber photometry data. *Pharmacol Biochem Behav* 2021; 201: 173093.
15. Lu L, Uejima JL, Gray SM, Bossert JM, Shaham Y. Systemic and central amygdala injections of the mGluR(2/3) agonist LY379268 attenuate the expression of incubation of cocaine craving. *Biol Psychiatry* 2007; 61(5): 591–598.
16. Lu L, Wang X, Wu P, Xu C, Zhao M, Morales M *et al.* Role of ventral tegmental area glial cell line-derived neurotrophic factor in incubation of cocaine craving. *Biol Psychiatry* 2009; 66(2): 137–145.
17. Wang C, Yue H, Hu Z, Shen Y, Ma J, Li J *et al.* Microglia mediate forgetting via complement-dependent synaptic elimination. *Science* 2020; 367(6478): 688–694.
18. Paxinos G, Watson C. *The rat brain in stereotaxic coordinates*. Academic Press 2007.
19. Sebastian V, Estil JB, Chen D, Schrott LM, Serrano PA. Acute physiological stress promotes clustering of synaptic markers and alters spine morphology in the hippocampus. *PLoS One* 2013; 8(10): e79077.
20. Muller CP, Quednow BB, Lourdasamy A, Kornhuber J, Schumann G, Giese KP. CaM Kinases: From memories to addiction. *Trends Pharmacol Sci* 2016; 37(2): 153–166.
21. Shin CB, Templeton TJ, Chiu AS, Kim J, Gable ES, Vieira PA *et al.* Endogenous glutamate within the prelimbic and infralimbic cortices regulates the incubation of cocaine-seeking in rats. *Neuropharmacology* 2018; 128: 293–300.
22. DeNardo LA, Liu CD, Allen WE, Adams EL, Friedmann D, Fu L *et al.* Temporal evolution of cortical ensembles promoting remote memory retrieval. *Nat Neurosci* 2019; 22(3): 460–469.

23. Xia F, Richards BA, Tran MM, Josselyn SA, Takehara-Nishiuchi K, Frankland PW. Parvalbumin-positive interneurons mediate neocortical-hippocampal interactions that are necessary for memory consolidation. *Elife* 2017; 6: 1–25.
24. Lesburgueres E, Gobbo OL, Alaux-Cantin S, Hambucken A, Trifilieff P, Bontempi B. Early tagging of cortical networks is required for the formation of enduring associative memory. *Science* 2011; 331(6019): 924–928.
25. Gomez JL, Bonaventura J, Lesniak W, Mathews WB, Sysa-Shah P, Rodriguez LA *et al.* Chemogenetics revealed: DREADD occupancy and activation via converted clozapine. *Science* 2017; 357(6350): 503–507.
26. Tye KM, Janak PH. Amygdala neurons differentially encode motivation and reinforcement. *J Neurosci* 2007; 27(15): 3937–3945.
27. Klavir O, Prigge M, Sarel A, Paz R, Yizhar O. Manipulating fear associations via optogenetic modulation of amygdala inputs to prefrontal cortex. *Nat Neurosci* 2017; 20(6): 836–844.
28. Carelli RM, Williams JG, Hollander JA. Basolateral amygdala neurons encode cocaine self-administration and cocaine-associated cues. *J Neurosci* 2003; 23(23): 8204–8211.
29. Josselyn SA, Tonegawa S. Memory engrams: Recalling the past and imagining the future. *Science* 2020; 367(6473): eaaw4325.
30. Ebrahimi S, Okabe S. Structural dynamics of dendritic spines: molecular composition, geometry and functional regulation. *Biochim Biophys Acta* 2014; 1838(10): 2391–2398.
31. Gawin FH KH. Abstinence symptomatology and psychiatric diagnosis in cocaine abusers. *Arch Gen Psychiatry* 1986; 43: 107–113.
32. Grimm JW, Hope BT, Wise RA, Shaham Y. Incubation of cocaine craving after withdrawal. *Nature* 2001; 412(6843): 141–142.
33. Liu X, Yuan K, Lu T, Lin X, Zheng W, Xue Y *et al.* Preventing incubation of drug craving to treat drug relapse: from bench to bedside. *Mol Psychiatry* 2023; 28(4): 1415–1429.
34. Bedi G, Preston KL, Epstein DH, Heishman SJ, Marrone GF, Shaham Y *et al.* Incubation of cue-induced cigarette craving during abstinence in human smokers. *Biol Psychiatry* 2011; 69(7): 708–711.
35. Wang G, Shi J, Chen N, Xu L, Li J, Li P *et al.* Effects of length of abstinence on decision-making and craving in methamphetamine abusers. *PLoS One* 2013; 8(7): 1–7.
36. Li P, Wu P, Xin X, Fan YL, Wang GB, Wang F *et al.* Incubation of alcohol craving during abstinence in patients with alcohol dependence. *Addict Biol* 2015; 20(3): 513–522.
37. Parvaz MA, Moeller SJ, Goldstein RZ. Incubation of cue-induced craving in adults addicted to cocaine measured by electroencephalography. *JAMA Psychiatry* 2016; 73(11): 1127–1134.
38. Grant S, London ED, Newlin DB, Villemagne VL, Liu X, Contoreggi C *et al.* Activation of memory circuits during cue-elicited cocaine craving. *Proc Natl Acad Sci U S A* 1996; 93(21): 12040–12045.

39. Yue JL, Yuan K, Bao YP, Meng SQ, Shi L, Fang Q *et al*. The effect of a methadone-initiated memory reconsolidation updating procedure in opioid use disorder: A translational study. *EBioMedicine* 2022; 85: 104283.
40. Tronson NC, Taylor JR. Addiction: A drug-induced disorder of memory reconsolidation. *Curr Opin Neurobiol* 2013; 23(4): 573–580.
41. Grimm JW, Harkness JH, Ratliff C, Barnes J, North K, Collins S. Effects of systemic or nucleus accumbens-directed dopamine D1 receptor antagonism on sucrose seeking in rats. *Psychopharmacology (Berl)* 2011; 216(2): 219–233.
42. Pickens CL, Golden SA, Adams-Deutsch T, Nair SG, Shaham Y. Long-lasting incubation of conditioned fear in rats. *Biol Psychiatry* 2009; 65(10): 881–886.
43. Matos MR, Visser E, Kramvis I, van der Loo RJ, Gebuis T, Zalm R *et al*. Memory strength gates the involvement of a CREB-dependent cortical fear engram in remote memory. *Nat Commun* 2019; 10(1): 2315.
44. Gueye AB, Allain F, Samaha AN. Intermittent intake of rapid cocaine injections promotes the risk of relapse and increases mesocorticolimbic BDNF levels during abstinence. *Neuropsychopharmacology* 2019; 44(6): 1027–1035.
45. Markou A, Li J, Tse K, Li X. Cue-induced nicotine-seeking behavior after withdrawal with or without extinction in rats. *Addict Biol* 2018; 23(1): 111–119.
46. Hyman SE, Malenka RC. Addiction and the brain: The neurobiology of compulsion and its persistence. *Nat Rev Neurosci* 2001; 2(10): 695–703.
47. Yehuda R, Hoge CW, McFarlane AC, Vermetten E, Lanius RA, Nievergelt CM *et al*. Post-traumatic stress disorder. *Nat Rev Dis Primers* 2015; 1: 15057.
48. Squire LR, Genzel L, Wixted JT, Morris RG. Memory consolidation. *Cold Spring Harb Perspect Biol* 2015; 7(8): a021766.
49. West EA, Saddoris MP, Kerfoot EC, Carelli RM. Prelimbic and infralimbic cortical regions differentially encode cocaine-associated stimuli and cocaine-seeking before and following abstinence. *Eur J Neurosci* 2014; 39(11): 1891–1902.
50. Everitt BJ, Robbins TW. Neural systems of reinforcement for drug addiction: From actions to habits to compulsion. *Nat Neurosci* 2005; 8(11): 1481–1489.
51. Janak PH, Tye KM. From circuits to behaviour in the amygdala. *Nature* 2015; 517(7534): 284–292.
52. Lu L, Hope BT, Dempsey J, Liu SY, Bossert JM, Shaham Y. Central amygdala ERK signaling pathway is critical to incubation of cocaine craving. *Nat Neurosci* 2005; 8(2): 212–219.
53. Tonegawa S, Morrissey MD, Kitamura T. The role of engram cells in the systems consolidation of memory. *Nat Rev Neurosci* 2018; 19(8): 485–498.
54. Barrientos C, Knowland D, Wu MMJ, Lilascharoen V, Huang KW, Malenka RC *et al*. Cocaine-Induced Structural Plasticity in Input Regions to Distinct Cell Types in Nucleus Accumbens. *Biol Psychiatry* 2018; 84(12): 893–904.

55. Mashhoon Y, Wells AM, Kantak KM. Interaction of the rostral basolateral amygdala and prelimbic prefrontal cortex in regulating reinstatement of cocaine-seeking behavior. *Pharmacol Biochem Behav* 2010; 96(3): 347–353.
56. Ghazizadeh A, Hong S, Hikosaka O. Prefrontal cortex represents long-term memory of object values for months. *Curr Biol* 2018; 28(14): 2206–2217
57. Ma YY, Lee BR, Wang X, Guo C, Liu L, Cui R *et al*. Bidirectional modulation of incubation of cocaine craving by silent synapse-based remodeling of prefrontal cortex to accumbens projections. *Neuron* 2014; 83(6): 1453–1467.

Figures

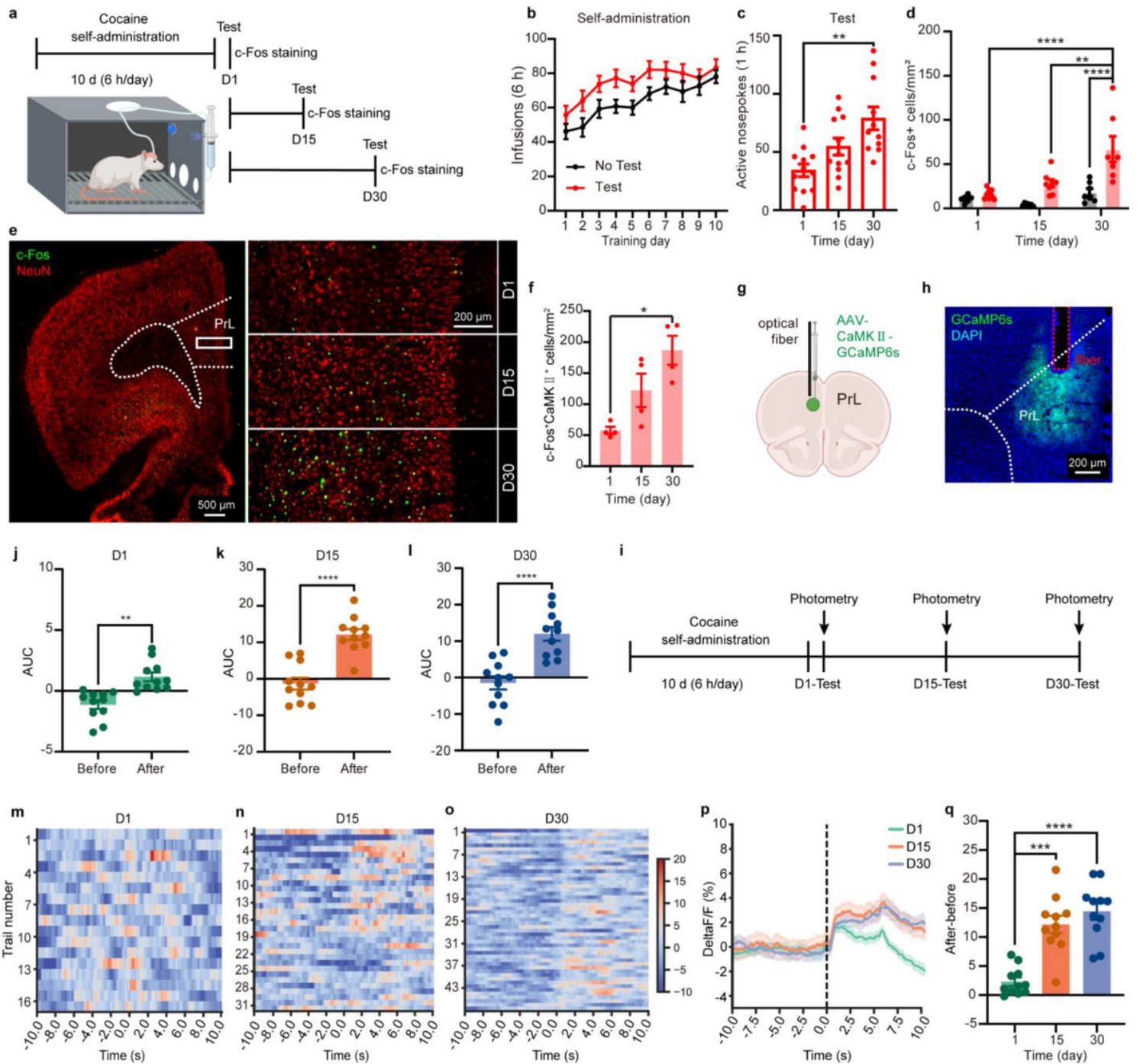


Figure 1

PrL CaMKII neuron activity time-dependently increases along with the enhancement of remote cocaine memory. **a**, Experimental timeline. After 10 days of cocaine self-administration, the rats underwent a 1 h memory test on day 1, 15, or 30. After 1h following test, rats were perfused for the immunofluorescence of c-Fos. **b**, Number of cocaine infusions during the 10-day training. **c**, Nosepokes on day 30 were higher than on day 1 ($n = 11-12$ rats). **d**, The density of c-Fos positive cells in the PrL increased on day 30 after the test. The number of PrL c-Fos positive cells after the test on day 30 was higher than on days 1 and 15, respectively ($n = 6-8$ rats). **e**, Representative images of c-Fos expression in the PrL in the test group.

Green: c-Fos. Red: NeuN. Scale bar: 500 μm , 200 μm . **f**, Cells co-labeled with c-Fos and CaMK in the PrL was higher after the test on day 30 than on day 1 ($n = 4$ rats). **g**, AAV-CaMK -GCaMP6s was injected into the PrL, along with the optical fiber in the same location. **h**, Representative photo of GCaMP6s expression in the PrL. Green: GCaMP6s. Blue: DAPI. Scale bar: 200 μm . **i**, Experimental timeline. After 10 days training, fiber photometry was performed during the memory test on day 1, 15, and 30. **j-l**, Area under curve (AUC) of PrL CaMK neuron Ca^{2+} signals increased after cue onset (0-10 s) compared with baseline (-10 to 0 s) on day 1 (**j**), day 15 (**k**), and day 30 (**l**) ($n = 11$ rats). **m-o**, Trial-by-trial heatmap representations of Ca^{2+} signals during the memory test on day 1 (**m**), day 15 (**n**), and day 30 (**o**). **p**, Peri-event plot of average Ca^{2+} signals aligned to cue exposure from day 1 to day 30. **q**, The AUC change (after-before) was enhanced on day 15 and day 30 compared with day 1. $*P 0.05$, $**P 0.01$, $***P 0.001$, $****P 0.0001$. The data are expressed as the mean \pm SEM. Details of the statistical analyses are shown in Supplementary Table 1-3.

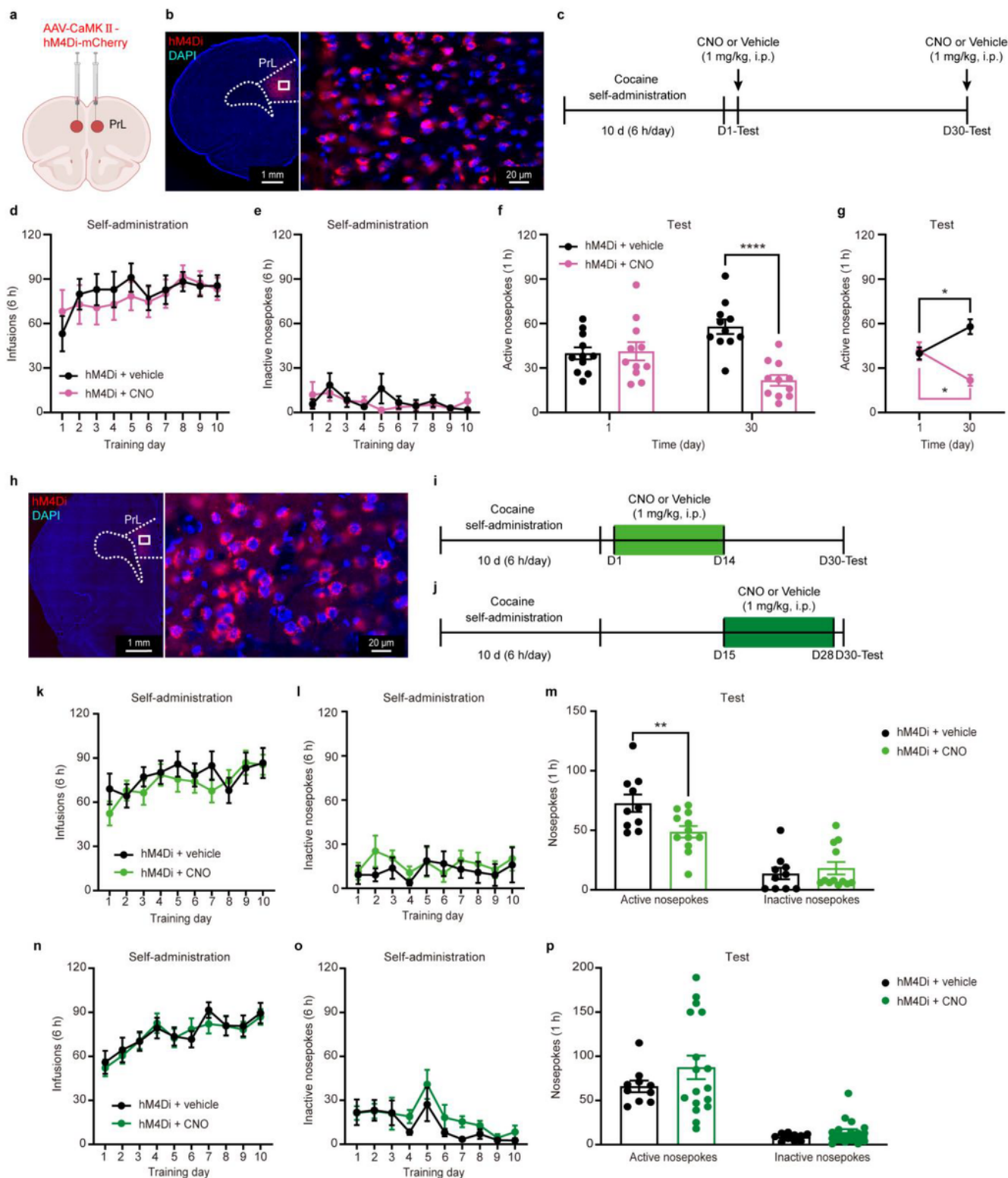


Figure 2

Inhibition of PrL CaMK neurons prevents the enhancement and consolidation of remote cocaine memory. **a**, AAV-CaMK II-hM4Di-mCherry was injected in the PrL. **b**, Representative photograph of hM4Di expression in the PrL. Red: hM4Di-mCherry. Blue: DAPI. Scale bar: 1 mm, 20 μ m. **c**, Experimental timeline. After 10 days of training, the rats underwent the memory test on day 1 and day 30, along with a CNO or vehicle (1 mg/kg, i.p.) injection 30 min before each test. **d,e**, Number of cocaine infusions (**d**) and inactive

nosepokes (**e**) during the 10 days of training. **f**, The chemogenetic inhibition of PrL CaMK neurons only reduced active nosepekes on day 30 (n = 11 rats). **g**, In rats receiving a CNO administration, the number of nosepekes on day 30 was less than on day 1. **h**, Representative photographs of hM4Di-mCherry expression in the PrL. Red: mCherry. Blue: DAPI. Scale bar: 1 mm, 20 μ m. **i,j**, Experimental timeline of chronic CNO or vehicle (1 mg/kg, i.p.) administration from day 1 to day 14 (**i**) or from day 15 to day 28 (**j**). **k,l**, Number of cocaine infusions (**k**) and inactive nosepekes (**l**) during the 10 days of self-administration training. **m**, The chronic inhibition of PrL CaMK neurons from day 1 to day 14 post training attenuated active nosepekes on day 30 (n = 10-12 rats). **n,o**, Number of cocaine infusions (**n**) and inactive nosepekes (**o**) during the 10 days of self-administration training. **p**, The chronic inhibition of PrL CaMK neurons from day 15 to day 28 post training had no influence on active nosepekes on day 30 (n = 10-17 rats). **P* 0.05, ***P* 0.01, *****P* 0.0001. The data are expressed as the mean \pm SEM. Details of the statistical analyses are showed in Supplementary Table 1.

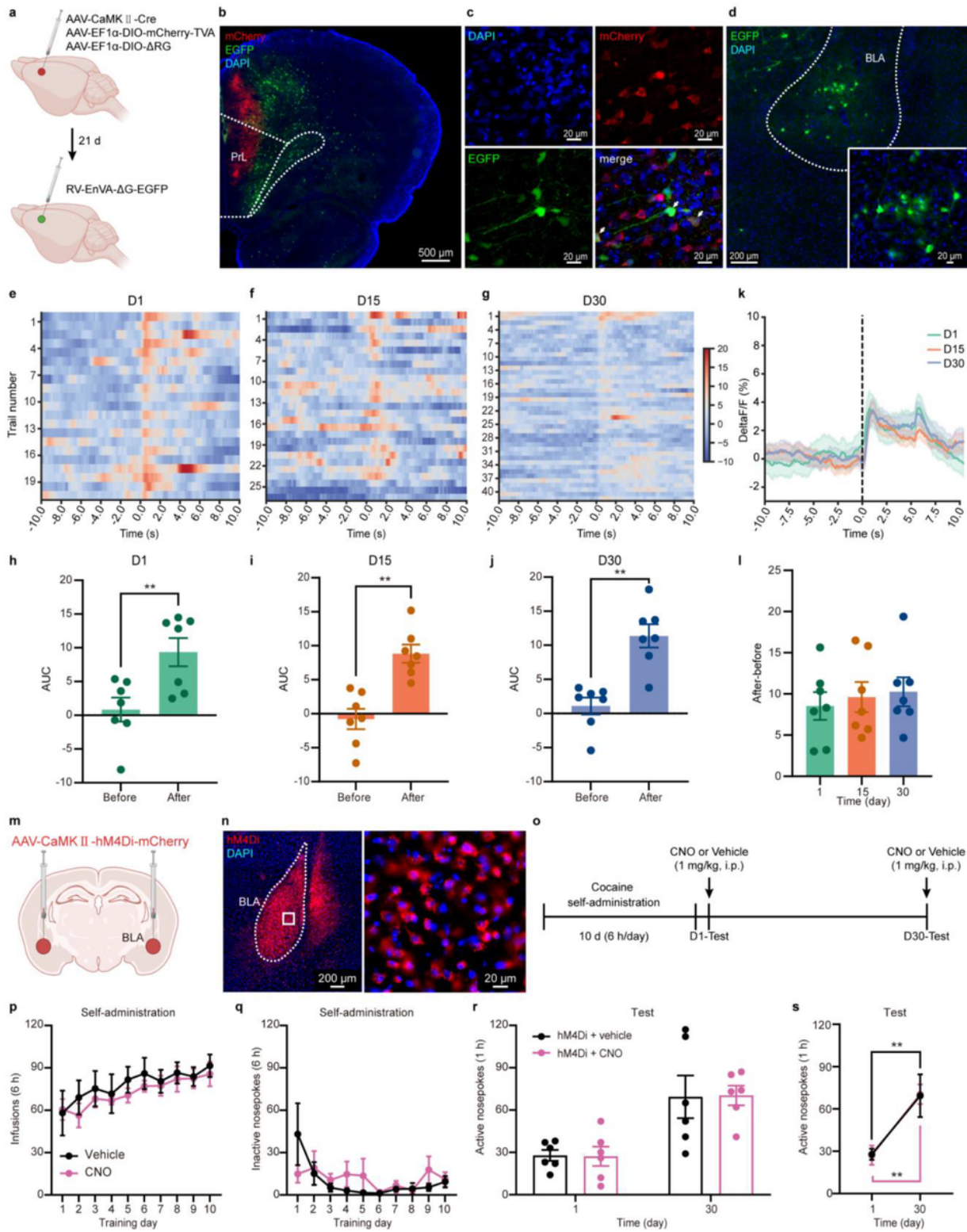


Figure 3

Enhancement of remote cocaine memory does not require BLA CaMK neurons. **a**, Experimental timeline. To trace the upstream input to PrL CaMK neurons, an AAV expressing Cre under the CaMK promoter was co-injected with AAV-EF1 α -DIO-mCherry-TVA and AAV-EF1 α -DIO- Δ RG in the PrL. 21 days later, RV-EnVA- Δ G-EGFP was injected in the same location. Starter neurons are identified according to the co-expression of mCherry and RV-EGFP. Input neurons only express RV-EGFP. **b,c**, Representative images of

starter neurons in the PrL which co-expressed mCherry and EGFP at scales of 500 μm (**b**) and 20 μm (**c**). White arrowheads: true starter neurons. Red: mCherry. Green: EGFP. Blue: DAPI. **d**, RV-EGFP labeled input neurons in the BLA at scales of 200 μm scale (**d**) and 20 μm (**d**, inset). Green: EGFP. Blue: DAPI. **e-g**, Trial-by-trial heatmap representations of the Ca^{2+} signals in BLA CaMK neurons during the memory test on day 1 (**e**), day 15 (**f**), and day 30 (**g**) ($n = 7$ rats). **h-g**, The AUC of BLA CaMK neuron Ca^{2+} signals increased after cue onset (0-10 s) compared with before cue exposure (-10 to 0 s) on day 1 (**h**), day 15 (**i**), and day 30 (**g**). **k**, Peri-event plot of average Ca^{2+} signals aligned to cue exposure from day 1 to day 30. **l**, The AUC change (after-before) had no change across test days. **m**, AAV-CaMK -hM4Di-mCherry was injected in the BLA. **n**, Representative photograph of hM4Di expression in the BLA. Red: hM4Di-mCherry. Blue: DAPI. Scale bar: 200 μm , 20 μm . **o**, Experimental timeline. After 10 days of training, the rats underwent the memory test on day 1 and day 30, along with a CNO or vehicle (1 mg/kg, i.p.) injection 30 min before every test. **p,q**, Number of cocaine infusions (**p**) and inactive nose pokes (**q**) during the 10 days of self-administration training. **r**, The chemogenetic inhibition of BLA CaMK neurons did not influence active nose pokes ($n = 6$ rats). **s**, In rats receiving a CNO or vehicle injection, both active nose pokes increased on day 30 compared with day 1. ****** $P < 0.01$. The data are expressed as the mean \pm SEM. Details of the statistical analyses are shown in Supplementary Table 1 and 3.

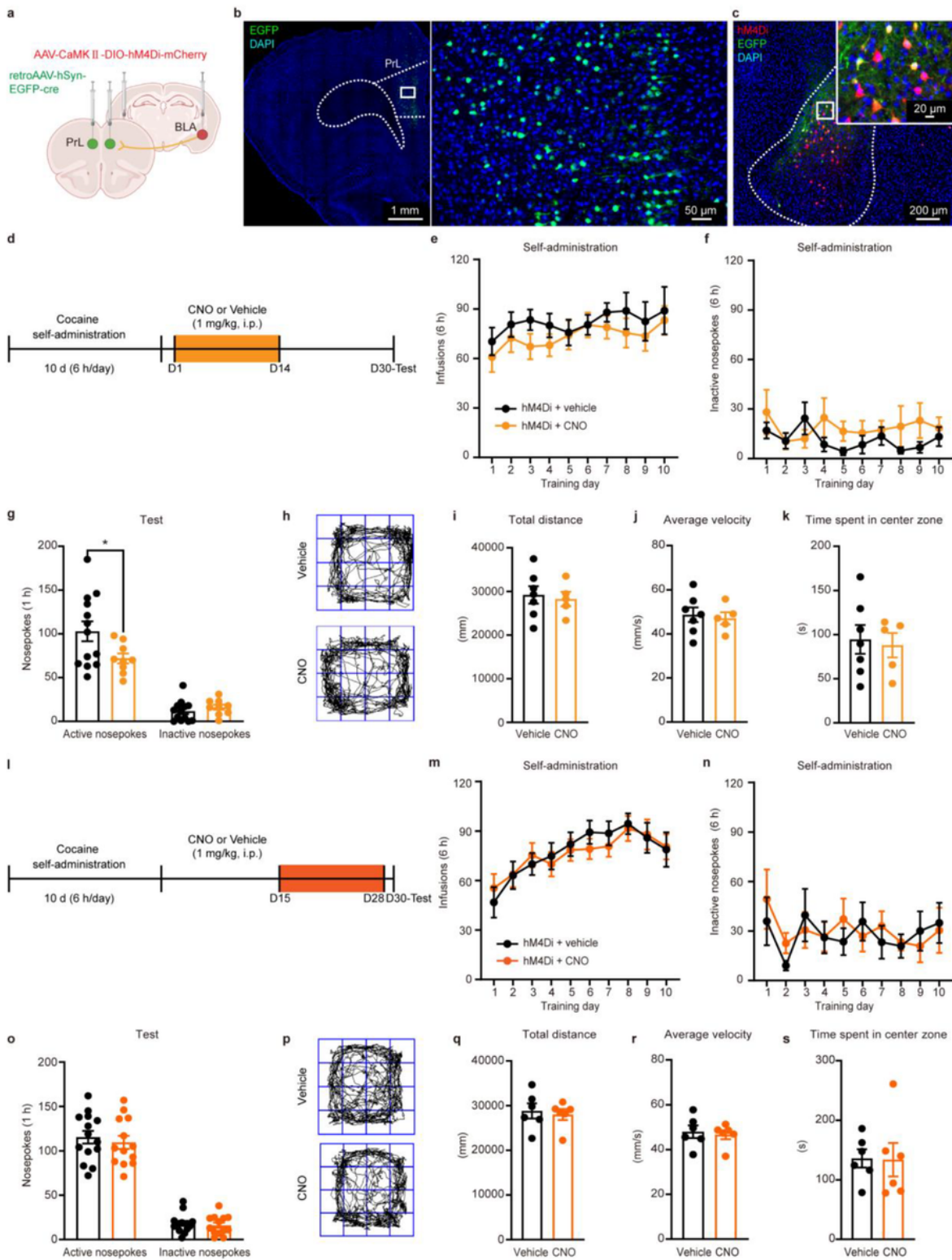


Figure 4

Chronic inhibition of the BLA-PrL circuit during the early period of consolidation prevents the enhancement of remote cocaine memory. **a**, AAV-CaMK II-DIO-hM4Di-mCherry was injected in the BLA, and retroAAV-hSyn-EGFP-cre was injected in the PrL. **b**, Representative images of EGFP-cre expression in the PrL. Green: EGFP. Blue: DAPI. Scale bar: 1 mm (left), 50 μ m (right). **c**, Representative images of hM4Di-mCherry expression in the BLA. Red: mCherry. Green: EGFP. Blue: DAPI. Scale bar: 200 μ m, 20 μ m (c,

inset). **d**, Experimental timeline of chronic CNO or vehicle (1 mg/kg, i.p.) administration from day 1 to day 14. **e,f**, Number of cocaine infusions (**e**) and inactive nose pokes (**f**) during the 10 days of self-administration training. **g**, Chronic inhibition of BLA-PrL circuit from day 1 to day 14 post training reduced the active nose pokes on day 30 (n = 9-13 rats). **h**, Trajectory path during the locomotor test in the CNO and vehicle groups which received injection during the early period (n = 5-7 rats). **i-k**, Total distance travelled (**i**), average velocity (**j**), and time spent in the center zone (**k**) did not change after chronic inhibition of the BLA-PrL projection during the early period. **l**, Experimental timeline of chronic CNO or vehicle (1 mg/kg, i.p.) administration from day 15 to day 28. **m,n**, Number of cocaine infusions (**m**) and inactive nose pokes (**n**) during the 10-day self-administration training. **o**, The number of active nose pokes on day 30 had no difference after chronically blocking the BLA-PrL circuit from day 15 to day 28 post-training (n = 13-14 rats). **p**, Trajectory path during the locomotor test in the CNO and vehicle groups which received injection during the late period (n = 5-6). **q-s**, Total distance travelled (**q**), average velocity (**r**), and time spent in the center zone (**s**) had no change after chronic inhibition of the BLA-PrL projection during late period. **P* 0.05. The data are expressed as the mean ± SEM. Details of the statistical analyses are shown in Supplementary Table 1.

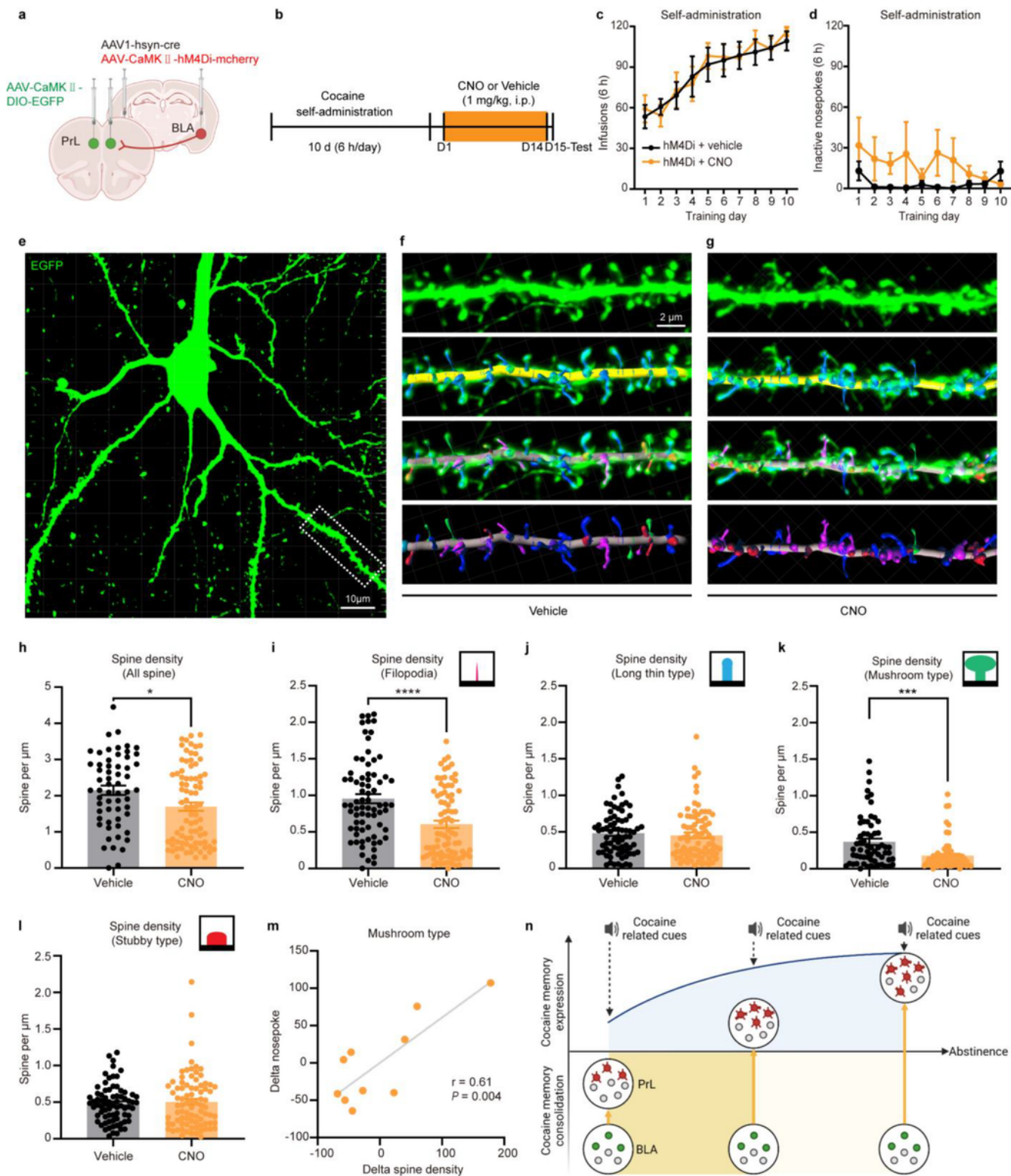


Figure 5

Chronic inhibition of the BLA input during the early period of consolidation impairs the dendritic spine density and maturation of PrL CaMK neurons. **a**, A mixture of AAV1-hSyn-Cre and AAV-CaMK II -hM4Di-mCherry was injected in the BLA, along with an injection of AAV-CaMK II -DIO-EGFP in the PrL. **b**, Experimental timeline of chronic CNO or vehicle (1 mg/kg, i.p.) administration from day 1 to day 14. **c,d**, Number of cocaine infusions (**c**) and inactive nosepokes (**d**) during the 10 days of self-administration

training. **e**, Representative image showing the EGFP expression in the PrL neurons receiving BLA input. Green: EGFP. Scale bar: 10 μm . **f,g**, Representative three-dimensional dendritic spine reconstruction and classification in the vehicle (**f**) and CNO (**g**) groups. Scale bar: 2 μm . Red: stubby type. Green: mushroom type. Blue: long thin type. Purple: filopodia type. **h-l**, Dendritic spine density for all spines (**h**) and stratified by filopodia (**i**), long thin type (**j**), mushroom type (**k**), and stubby type (**l**). Of these, a reduction of spine density was observed in all spines, filopodia-shaped spines, and mushroom-shaped spines ($n = 5$ rats). **m**, The delta density of mushroom-shaped spines showed a significant positive correlation with the delta nosepoke behaviors. **n**, Cocaine memory expression after cue exposure showed time-dependent enhancement, relying on the progressively increased and mature dendrite spine in PrL CaMK neuron. And these neurons required the sustained BLA input during memory consolidation, especially during the early period of system consolidation process. $*P < 0.05$, $***P < 0.001$, $****P < 0.0001$. The data are expressed as the mean \pm SEM. Details of the statistical analyses are shown in Supplementary Table 4.

Supplementary Files

This is a list of supplementary files associated with this preprint. Click to download.

- [FigureS1.pdf](#)
- [FigureS2.pdf](#)
- [FigureS3.pdf](#)
- [FigureS4.pdf](#)
- [FigureS5.pdf](#)
- [FigureS6.pdf](#)
- [FigureS7.pdf](#)
- [SupplementaryInformationJuly162023.docx](#)